

Selective measurement of NAPE-PLD activity via a PLA_{1/2}-resistant fluorogenic *N*-acyl-phosphatidylethanolamine analog

Jonah E. Zarrow^{1,2}, Jianhua Tian³, Brendan Dutter³, Kwangho Kim^{3,4}, Amanda C. Doran⁵, Gary A. Sulikowski^{2,3,4}, and Sean S. Davies^{2,3,*}

¹Chemical and Physical Biology Program, ²Department of Pharmacology, ³Vanderbilt Institute of Chemical Biology, and ⁴Department of Chemistry, Vanderbilt University, Nashville, TN, USA; ⁵Division of Cardiovascular Medicine, Department of Medicine, Vanderbilt University Medical Center, Nashville, TN, USA

Abstract *N*-acyl-phosphatidylethanolamine (NAPE)-hydrolyzing phospholipase D (NAPE-PLD) is a zinc metallohydrolase enzyme that converts NAPEs to bioactive *N*-acyl-ethanolamides. Altered NAPE-PLD activity may contribute to pathogenesis of obesity, diabetes, atherosclerosis, and neurological diseases. Selective measurement of NAPE-PLD activity is challenging, however, because of alternative phospholipase pathways for NAPE hydrolysis. Previous methods to measure NAPE-PLD activity involved addition of exogenous NAPE followed by TLC or LC/MS/MS, which are time and resource intensive. Recently, NAPE-PLD activity in cells has been assayed using the fluorogenic NAPE analogs PED-A1 and PED6, but these substrates also detect the activity of serine hydrolase-type lipases PLA₁ and PLA₂. To create a fluorescence assay that selectively measured cellular NAPE-PLD activity, we synthesized an analog of PED-A1 (flame-NAPE) where the *sn*-1 ester bond was replaced with an *N*-methyl amide to create resistance to PLA₁ hydrolysis. Recombinant NAPE-PLD produced fluorescence when incubated with either PED-A1 or flame-NAPE, whereas PLA₁ only produced fluorescence when incubated with PED-A1. Furthermore, fluorescence in HepG2 cells using PED-A1 could be partially blocked by either biotionol (a selective NAPE-PLD inhibitor) or tetrahydrolipstatin (an inhibitor of a broad spectrum of serine hydrolase-type lipases). In contrast, fluorescence assayed in HepG2 cells using flame-NAPE could only be blocked by biotionol. In multiple cell types, the phospholipase activity detected using flame-NAPE was significantly more sensitive to biotionol inhibition than that detected using PED-A1. Thus, using flame-NAPE to measure phospholipase activity provides a rapid and selective method to measure NAPE-PLD activity in cells and tissues.

Supplementary key words NAPE-PLD • phospholipase A1 • fluorescence • *N*-acyl-ethanolamide • *N*-acylphosphatidylethanolamide • biotionol • tetrahydrolipstatin • diabetes • atherosclerosis • nociception

N-acyl-phosphatidylethanolamine (NAPE) hydrolyzing phospholipase D (PLD) is a zinc metallohydrolase that catalyzes the final step of *N*-acyl-ethanolamide (NAE) biosynthesis (1–3). NAEs, including *N*-arachidonyl-ethanolamide (AEA), *N*-oleoyl-ethanolamide (OEA), and *N*-palmitoyl-ethanolamide (PEA), play critical roles in the regulation of food intake, inflammation, and nociception (4–11). Therefore, changes in NAPE-PLD activity may play an important role in the dysregulation of these processes that occur during cardiometabolic and neurological diseases. A facile assay to measure NAPE-PLD activity in cultured cells and tissues is needed to assess how changes in this activity may contribute to pathophysiology and to test the effectiveness of potential interventions targeting NAPE-PLD activity.

Current assay methods to measure NAPE-PLD activity are time consuming and/or lack selectivity for NAPE-PLD. NAPE-PLD activity has been most commonly measured by incubating radiolabeled NAPE with cells or cell homogenates, followed by extraction and separation of resulting NAE from NAPE by TLC (12). Depending on the cell type or tissue, this assay may not be selective for NAPE-PLD activity because it is usually carried out using radiolabeled NAPE with two *O*-acyl chains (diacyl-NAPE). Diacyl-NAPE can be hydrolyzed by alternative enzymatic pathways (6, 13, 14). For instance, alpha/beta-hydrolase-4 (ABHD4) exerts both PLA₁- and PLA₂-type phospholipase activity to hydrolyze diacyl-NAPEs to glycerophospho-NAEs (GP-NAEs) (6, 13, 15). These GP-NAEs can then be hydrolyzed to NAEs by the actions of glycerophosphodiesterases such as GDE1 and GDE4 (6, 15, 16). An assay that is more selective for NAPE-PLD activity can be achieved by using radiolabeled NAPE where the *sn*-1 and *sn*-2 ester bonds are replaced with ether bonds (diether-NAPE) to make it resistant to PLA_{1/2}-type phospholipases including ABHD4. The results observed with diether-NAPE differ from those with diacyl-NAPE

*For correspondence: Sean S. Davies, sean.davies@vanderbilt.edu.

(17–19). Regardless of which radiolabeled substrate is used, the use of radioisotopes requires specialized licensing, handling, and waste disposal, and TLC is labor intensive and time consuming. Another widely used approach to measure NAPE-PLD activity is to add nonradiolabeled *N*-C17:0-phosphatidylethanolamine (C17:0 NAPE) and then measure the resulting change in the ratio of this NAPE and its respective C17:0NAE product by LC/MS/MS (20–22). This LC/MS/MS assay is at least as labor intensive, time consuming, and expensive as the radioisotope method, and unless diether-C17:0 NAPE is used as substrate, also suffers from lack of selectivity for NAPE-PLD. Therefore, either of these two approaches are too cumbersome to measure NAPE-PLD activity in the large number of samples that are often needed for time-course studies or for screening of the effects of various stimuli or small molecules in cultured cells and tissues.

A more recent alternative approach to measure NAPE-PLD activity utilizes PED-A1 or PED6, two commercially available fluorogenic compounds designed to measure PLA₁ and PLA₂ activity, respectively (Fig. 1) (22–31). These two NAPE analogs are designed so that their hydrolysis by the intended phospholipase releases the dinitrophenol quencher

moiety to allow detection of the BODIPY fluorophore. While both PED-A1 and PED6 allow for rapid and inexpensive measurement of NAPE-PLD activity *in vitro*, their sensitivity to PLA₁ or PLA₂ hydrolysis limits their effectiveness for selectively measuring NAPE-PLD activity in cultured cells or tissues. We therefore designed and synthesized a PED-A1 analog (flame-NAPE) where the *sn*-1 ester bond was substituted with an *N*-methyl amide bond anticipated to be resistant to phospholipase hydrolysis (Fig. 1) and showed that this analog can be used to rapidly measure cellular NAPE-PLD activity without interference from cellular PLA₁ activity.

MATERIALS AND METHODS

Synthesis and purification of flame-NAPE

Synthesis and product verification for flame-NAPE were performed by the Molecular Design and Synthesis Center at Vanderbilt University as described in the supplemental data section. Briefly, commercially available (*R*)-glycerol acetone was selectively functionalized and protected to provide the central amino diol. This enabled the sequential introduction of the *sn*-2 chain, phosphate, ethanolamine, *N*-acyl chain, and *sn*-1 chain. The final product was isolated by flash

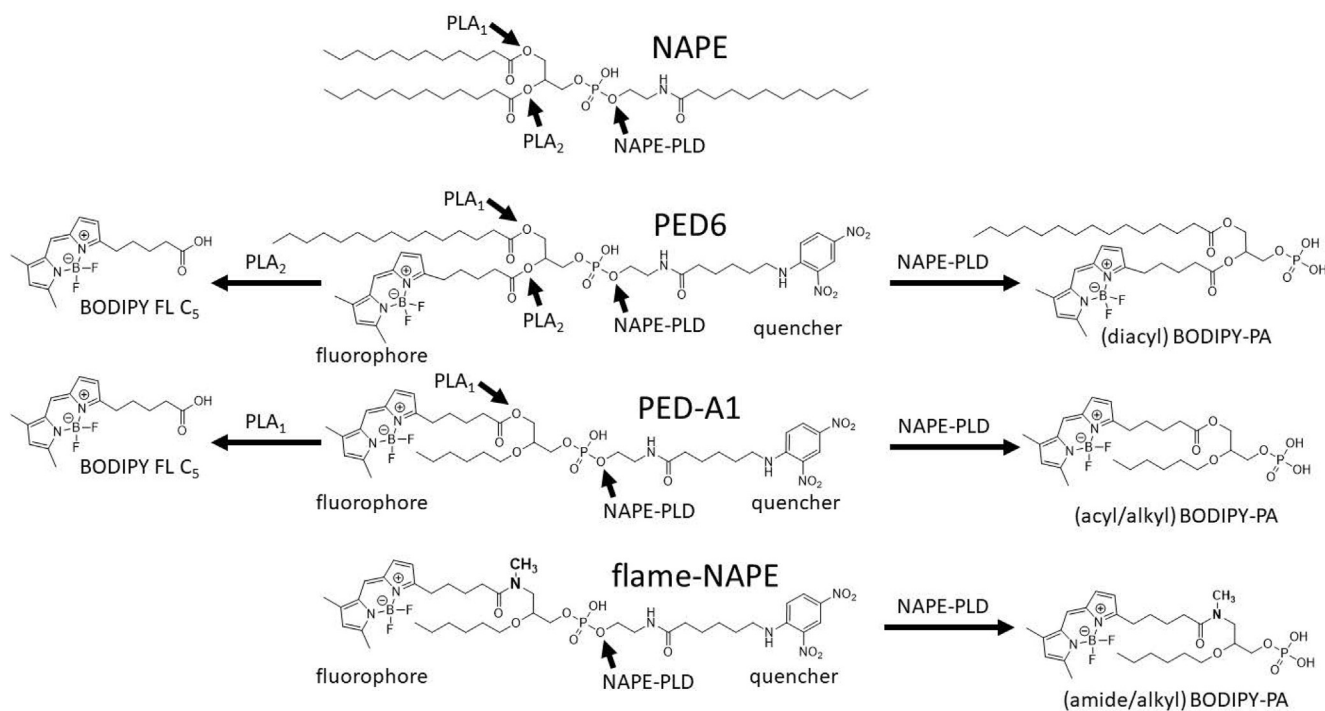


Fig. 1. Flame-NAPE is a fluorogenic NAPE analog designed to be resistant to PLA_{1/2} hydrolysis but sensitive to NAPE-PLD hydrolysis. Endogenous NAPE can be hydrolyzed by various phospholipases, including PLA₁, PLA₂, and NAPE-PLD. PED6 is a fluorogenic NAPE analog where the dinitrophenol moiety of the *N*-acyl chain quenches the fluorescence of the BODIPY moiety on the *sn*-2 acyl chain. PLA₂ hydrolysis of PED6 releases the quencher moiety to generate a fluorescent fatty acid (BODIPY FL C₅), whereas NAPE-PLD hydrolysis generates a fluorescent phosphatidic acid (diacyl BODIPY-PA). PLA₁ hydrolysis of PED6 releases the *sn*-1 fatty acid chain, but this does not generate fluorescence. PED-A1 is a fluorogenic NAPE where PLA₁ hydrolysis generates BODIPY-FL C₅, and NAPE-PLD hydrolysis generates a fluorescent phosphatidic acid (acyl/alkyl BODIPY-PA). The ether bond of the PED-A1 *sn*-2 chain is resistant to PLA₂ hydrolysis. Flame-NAPE was designed to enable selective detection of NAPE-PLD by substituting an *N*-methyl amide bond for the *sn*-1 ester bond of PED-A1, thereby making it resistant to both PLA₁ and PLA₂ hydrolysis while retaining sensitivity to NAPE-PLD hydrolysis.

chromatography to >95% purity as indicated by LC/MS and NMR analysis.

Acquisition of PED-A1 and flame-NAPE absorbance spectra

PED-A1 and flame-NAPE were prepared from dried stocks by dissolving in buffer containing 50 mM Tris-HCl, pH 8.0, ethanol, and DMSO (60:32:8 v/v/v), and the absorbance spectrum from 300 to 700 nm was recorded using an Eppendorf Biospectrometer kinetic UV-visible spectrometer.

In vitro assays for characterization of PED-A1 and flame-NAPE hydrolysis by NAPE-PLD and PLA₁

Recombinant mouse Nape-pld was expressed in *Escherichia coli* and purified as previously described (27). Purified *Aspergillus oryzae* Pla₁ was purchased commercially (Sigma; L3295). PED-A1 and flame-NAPE were prepared in buffer containing 50 mM Tris-HCl, pH 8.0, ethanol, and DMSO (60:32:8 v/v/v).

K_M determination. 55 μl of 50 mM Tris-HCl buffer (pH = 8) and 5 μl of 7% (w/v) *N*-octyl-β-D-glucoside solution (Millipore; 494459) was added to clear-bottom, black-walled, nontreated, 96-well plates (Thermo; 265301), followed by 5 μl of 73 μg/ml Nape-pld (final concentration of 4.56 μg/ml) or 5 μl of Tris-HCl buffer (for negative controls), and then 5 μl of test compound vehicle (1.6% DMSO [v/v] in Tris-HCl buffer) and incubated for 1 h at 37°C. To initiate the activity assay, 10 μl of ice-cold PED-A1 or flame-NAPE was added to every well with final concentration from 0 to 20 μM (six replicates per condition). Fluorescence (excitation/emission = 488/530 nm) was measured in a BioTek Synergy HI plate reader at 37°C. Reaction rate was measured as Δfluorescence from $t = 1$ to $t = 4$ min, $n = 6$, mean ± SEM. K_M values were calculated in GraphPad Prism 7.0 (Graphpad Software L.L.C.) using nonlinear regression (allosteric sigmoidal) and software; there was evidence of an inadequate model for the flame-NAPE regression ($F = 3.63$; $P = 0.0144$).

Determination of enzyme selectivity. 60 μl of Tris-HCl buffer was added to wells of a clear-bottom, black-walled, nontreated, 96-well plate, followed by 5 μl of Nape-pld (final concentration of 4.56 μg/ml), *A. oryzae* PLA₁ (final concentration of 34.6 U/ml), or Tris-HCl buffer (negative control). About 5 μl of 7% (w/v) *N*-octyl-β-D-glucoside solution was added to the wells that received Nape-pld and 5 μl of Tris-HCl buffer to wells that received PLA₁ or the negative control. After 1 h of incubation at 37°C, 10 μl of ice-cold substrate was added (final concentration of 4 μM), and fluorescence was measured as aforementioned. Background fluorescence in the absence of phospholipase was subtracted from all groups.

Measurement of phospholipase activity in cells using flame-NAPE and PED-A1

HepG2, human embryonic kidney 293 (HEK293), 3T3-L1, and Caco-2 cells (human colon carcinoma cell lines) were purchased from ATCC (HB-8065, CRL-1573, CL-173, and HTB-37, respectively). Bone marrow progenitors were obtained from 8- to 12-week-old C57BL6/J mice. These progenitors were cultured using a previously published method to yield the bone marrow-derived macrophages (BMDMs) (32). The base cell media for all cell assays were DMEM with 4.5 g/l glucose, 1 mM sodium pyruvate, and 4 mM L-glutamine. For

the growth of HEK293 and 3T3-L1 cells, phenol red and 10% (v/v) heat-inactivated FBS were added to base media. For Caco-2 cell growth, phenol red and 20% (v/v) heat-inactivated FBS were added to base media. For the assay, all cells were plated at 20,000 cells/well in clear-bottom, black-walled, tissue culture-treated, 96-well plates; negative control wells had no cells added. After the cells reached ~90% confluency, the growth media were removed, and 100 μl/well of treatment media (see later) added, incubated for 1 h at 37°C, then 5 μl of 84 μM PED-A1 or flame NAPE in Tris-HCl/ethanol/DMSO (60:32:8 v/v/v) added to each of the wells (final concentration of 4 μM). For the primary HepG2 cell studies, the treatment media were base media with either NAPE-PLD inhibitor bithionol (Bith; final concentration of 15 μM), the pan-serine hydrolase lipase inhibitor tetrahydrolipstatin (THL; final concentration of 10 μM), both, or vehicle (DMSO); all contained 0.71% v/v DMSO final. For the supplemental HepG2 cell study, the treatment media were base media with either 15 μM Bith, 33 μM LEI-401 (Cayman Chemicals), both, or vehicle (DMSO); all contained 1.7% v/v DMSO final. For assays with HEK293, 3T3-L1, BMDM, or Caco-2 cells, the inhibitor media were base media with either Bith (final concentration of 15 μM) or vehicle (DMSO); with the concentration of DMSO in all assays being 0.016% v/v final. For all cellular experiments, fluorescence (excitation/emission = 488/530 nm) was measured at 1 min intervals in a BioTek Synergy HI plate reader at 37°C. After the initial study in HepG2 cells, subsequent studies used the fluorescence values at 10 min for analysis. Final values were reported as substrate-normalized cellular fluorescence. To calculate this value, cellular fluorescence was first calculated as the fluorescence in the well measured at 10 min minus the average fluorescence of the wells with the appropriate substrate, but no cells (background fluorescence) were measured at 10 min. This cellular fluorescence value was then normalized by dividing this value by the average cellular fluorescence value for vehicle (DMSO only)-treated cells and multiplying by 100%. Each experiment was carried out on at least two separate days, and the normalized values from separate days were combined. For HepG2 cells, background fluorescence at 10 min for PED-A1 and flame-NAPE was typically 12% and 21%, respectively, of the raw fluorescence for vehicle-treated HepG2 cells. At the 10 min time point, the average raw fluorescence measured in vehicle-treated HepG2 cells with flame-NAPE was 66% that of similarly treated cells with PED-A1. For HEK293, 3T3-L1, BMDM, and Caco-2 cells where PED-A1 was used as substrate, the average background fluorescence (wells without cells) at the 10 min end point was 20%, 23%, 23%, and 19%, respectively, of the raw fluorescence of vehicle-treated cells. For HEK293, 3T3-L1, BMDM, and Caco-2 cells where flame-NAPE was used as substrate, the background fluorescence (wells without cells) at the 10 min end point was 24%, 34%, 33%, and 22%, respectively, of total raw fluorescence of vehicle-treated cells. The average raw fluorescence at 10 min end point for vehicle-treated HEK293, 3T3-L1, BMDM, and Caco-2 cells when 4 μM flame-NAPE was used as substrate was 89%, 94%, 76%, and 92%, respectively, of the raw fluorescence when 4 μM PED-A1 was used as substrate.

RESULTS

Synthesis of flame-NAPE and characterization as NAPE-PLD substrate

To create a fluorogenic NAPE analog likely to be resistant to both PLA₁ and PLA₂ hydrolysis for our

assay, we sought to generate a PED-A1 analog where the *sn*-1 ester bond of PED-A1 was substituted with either an ether bond or an *N*-methyl amide bond. Initial attempts to synthesize an ether bond analog gave poor results, so we focused our synthesis efforts on the *N*-methyl amide substitution. Details for synthesis of this *fluorogenic amide* NAPE analog (flame-NAPE; Fig. 1) are given in the supplemental data section. The absorbance spectrums of flame-NAPE closely matched those of PED-A1 both prior to and after hydrolysis with Nape-pld (Fig. 2A), confirming the presence of the BODIPY group (peak absorbance at 505 ± 3 nm) and the dinitrophenyl group (peak absorbance at 348 ± 4 nm) for flame-NAPE. Without hydrolysis with Nape-pld, no fluorescence emission was detected for either flame-NAPE or PED-A1 when exciting at 488 nm. Hydrolysis with Nape-pld resulted in similar fluorescence emission spectrum for flame-NAPE and PED-A1 (Fig. 2A). To assess the effect of

the *N*-methyl amide bond substitution on substrate hydrolysis by Nape-pld, varying concentrations of flame-NAPE or PED-A1 were incubated with recombinant mouse Nape-pld, and the resulting rate of fluorescence generation was measured. These studies showed that the K_m of flame-NAPE ($9.2 \mu\text{M}$) was reasonably similar to that of PED-A1 ($4.0 \mu\text{M}$) (Fig. 2B), consistent with flame-NAPE being a robust Nape-pld substrate.

Flame-NAPE is resistant to PLA₁ hydrolysis in vitro

Resistance to hydrolysis by enzymes with PLA₁-type activity would be a major advantage of flame-NAPE over the existing activity probe PED-A1. As expected, PED-A1 was readily hydrolyzed to a fluorescent product (excitation of 488/emission of 530 nm) by 50 min incubation with either purified *A. oryzae* Pla₁ or recombinant Nape-pld (Fig. 3A). In contrast, flame-NAPE could be hydrolyzed to a fluorescent

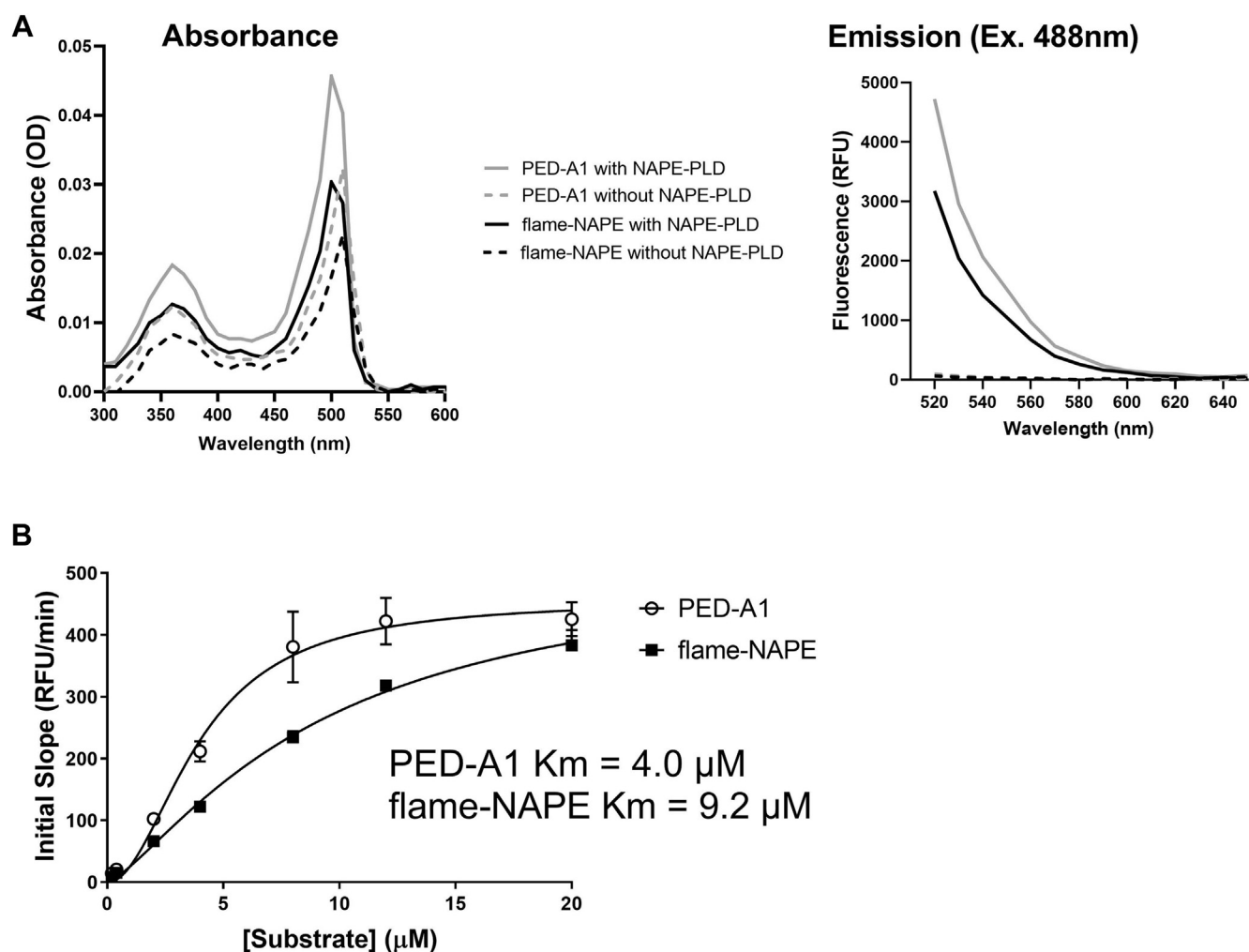


Fig. 2. PED-A1 and flame-NAPE share similar spectrometric and Nape-pld utilization properties. A: UV-visible absorbance and fluorescence emission spectrum of PED-A1 and flame-NAPE with and without incubation with Nape-pld. Excitation at 488 nm was used to determine fluorescence emission spectrum. B: Michaelis-Menten plot for hydrolysis of PED-A1 ($K_M = 4.0 \mu\text{M}$) and flame-NAPE ($K_M = 9.2 \mu\text{M}$) by recombinant murine Nape-pld ($4.56 \mu\text{g}/\text{ml}$). Fluorescence excitation 488 nm and emission 530 nm. Each point represents mean \pm SEM, $n = 6$.

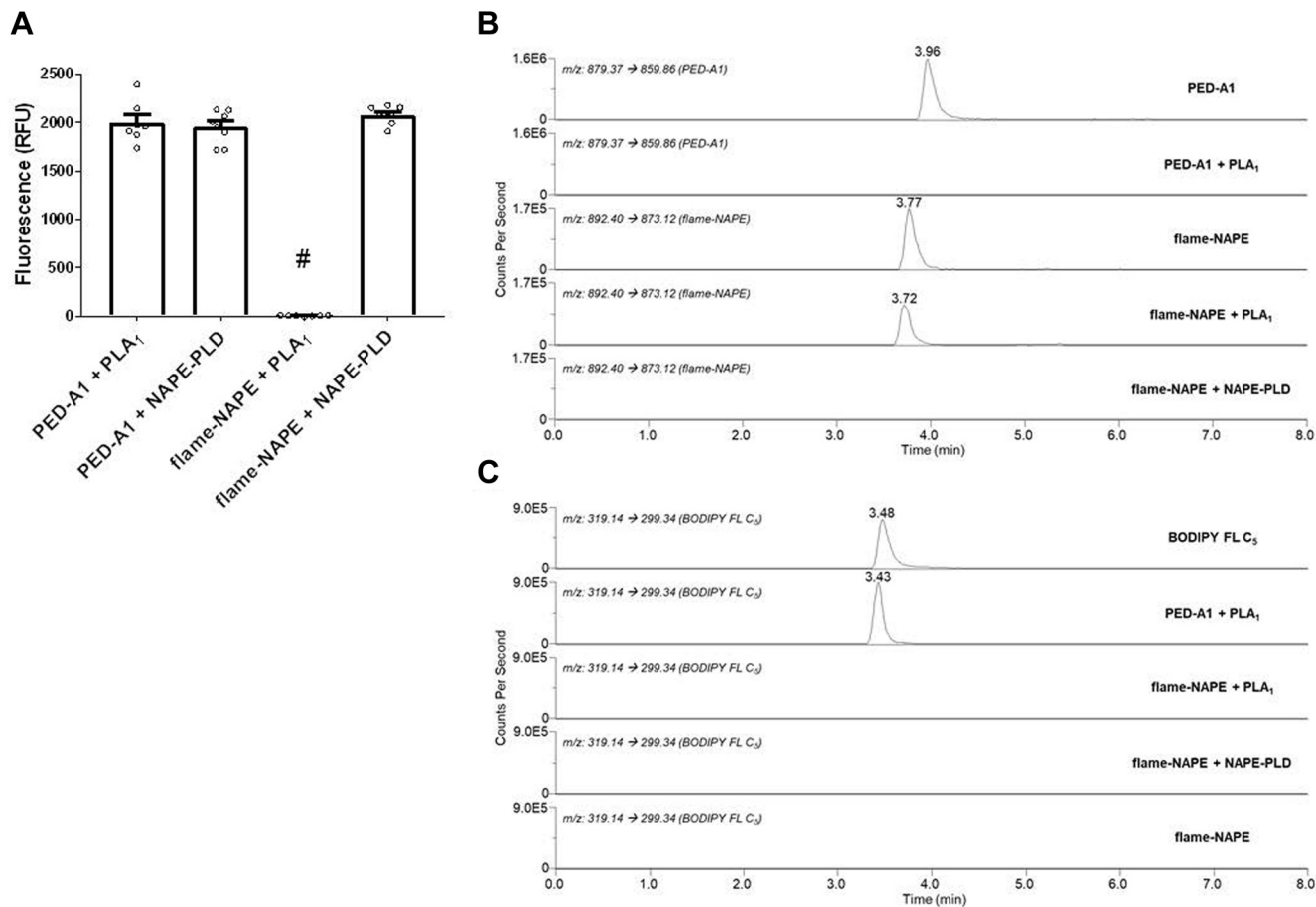


Fig. 3. Flame-NAPE is a fluorogenic substrate for Nape-pld, but not Pla₁, whereas PED-A1 is a fluorogenic substrate for both phospholipases. PED-A1 and flame-NAPE were incubated in vitro with either purified Pla₁ from *Aspergillus oryzae* or recombinant murine Nape-pld, and the extent of hydrolysis was measured by fluorescence and LC/MS/MS. **A:** Fluorescence (excitation of 488 nm/emission of 530 nm) generated by phospholipase treatment with PED-A1 or flame-NAPE. One-way ANOVA; $P = 0.0310$; Tukey multiple comparisons, # $P < 0.0001$ versus the other treatments. **B:** Representative multiple reaction monitoring chromatographs for unhydrolyzed PED-A1 (m/z 879.1 \rightarrow 859.9) and unhydrolyzed flame-NAPE (m/z 892.4 \rightarrow 873.1). **C:** Representative multiple reaction monitoring chromatographs for BODIPY FL C₅ (m/z 319.1 \rightarrow 299.3).

product only by Nape-pld and not by purified *A. oryzae* Pla₁ (Fig. 3A). To confirm that the lack of fluorescence after incubation with Pla₁ was the result of resistance of the substrate to hydrolysis, we developed an LC/MS/MS multiple reaction monitoring method to measure intact PED-A1 (m/z 879.4 \rightarrow m/z 859.9) or flame-NAPE (m/z 892.4 \rightarrow m/z 873.1) and the expected Pla₁ hydrolysis product BODIPY-FL C₅ (m/z 319.1 \rightarrow m/z 299.3) and used this method to analyze the products of the aforementioned experiment. Incubation of PED-A1 with purified *A. oryzae* Pla₁ for 50 min resulted in complete loss of LC/MS/MS signal for intact PED-A1 (Fig. 3B) and the formation of robust LC/MS/MS signal for BODIPY FL C₅ (Fig. 3C). In contrast, incubation of flame-NAPE with purified *A. oryzae* Pla₁ had little effect on the LC/MS/MS signal for intact flame-NAPE and failed to generate any signal for BODIPY FL C₅ (Fig. 3C). Incubation of flame-NAPE with recombinant mouse NAPE-PLD resulted in complete loss of signal for intact flame-NAPE (and no formation of BODIPY FL

C₅), consistent with flame-NAPE being a selective Nape-pld substrate.

Phospholipase activity assayed using flame-NAPE is insensitive to PLA₁ inhibition

In addition to their use to monitor NAPE-PLD activity in living cells, PED-A1 and PED6 have also been used extensively to measure PLA₁ and PLA₂ activity, respectively (22–31). Therefore, fluorescence measured with these probes may reflect multiple phospholipase activities. HepG2 cells are a human hepatocellular carcinoma cell line that express both hepatic lipase (which has significant PLA₁-type activity) and NAPE-PLD. To determine if using flame-NAPE in place of PED-A1 provided a more selective assay for NAPE-PLD activity in these cells, we investigated the sensitivity of the two substrates to inhibition of PLA₁ and NAPE-PLD. THL covalently reacts with the catalytic serine of a broad range of lipases including PLA₁s such as endothelial lipase and hepatic lipase (33–37). Because NAPE-PLD is a zinc metallohydrolase, rather than a serine

hydrolase, THL does not inhibit the activity of this phospholipase. We recently identified Bith as a potent and selective NAPE-PLD inhibitor (27). In the absence of these inhibitors, addition of either 4 μM PED-A1 or 4 μM flame-NAPE to HepG2 cells generated robust time-dependent increases in cellular fluorescence (total fluorescence minus average fluorescence of substrate in media without cells) indicative of phospholipase activity (Fig. 4). The fluorescence measured at the 50 min time point using 4 μM PED-A1 was 2.9-fold greater than fluorescence measured using 4 μM flame-NAPE. Treatment with 10 μM THL decreased PED-A1 cellular fluorescence compared with no inhibitor, particularly at time points greater than 10 min (Fig. 4A). Treatment with 15 μM Bith also decreased PED-A1 cellular fluorescence, and treatment with THL in addition to Bith further decreased PED-A1 cellular fluorescence (Fig. 4A). In contrast, while treatment with 15 μM Bith markedly decreased flame-NAPE cellular fluorescence, treatment with 10 μM THL had no effect on flame-NAPE cellular fluorescence (Fig. 4B). These results are consistent with PED-A1 cellular fluorescence reporting both NAPE-PLD and PLA₁ activity and flame-NAPE cellular fluorescence reporting NAPE-PLD activity but not PLA₁ activity. These results also suggest that using a relatively short time point (e.g., 10 min) as an end point makes PED-A1 cellular fluorescence more selective for NAPE-PLD than longer time points (e.g., 50 min) where PLA₁ activity much more significantly contributes to the signal.

The residual cellular fluorescence seen with flame-NAPE after 15 μM Bith treatment of the HepG2 cells (27% of vehicle-treated cells) likely reflects incomplete NAPE-PLD inhibition. The IC₉₅ for Bith using recombinant Nape-pld is 62.0 μM (27), but 60 μM Bith is cytotoxic to HepG2 cells (supplemental Fig. S2). Residual flame-NAPE cellular fluorescence when combining 15 μM Bith with another NAPE-PLD

inhibitor (33 μM LEI-401) (22) was only 10% (supplemental Fig. S3).

Flame-NAPE can be used to selectively measure NAPE-PLD activity in multiple cell types

NAPE-PLD has been implicated in playing key roles in adipocytes, kidney epithelial cells, intestinal enterocytes, and macrophages (7, 38–42). These cells express PLA₁s in addition to NAPE-PLD (43–46), so we sought to determine if flame-NAPE would report NAPE-PLD activity in these cell types more selectively than PED-A1. PED-A1 and flame-NAPE were incubated with cultured HEK293 epithelial cells, 3T3-L1 cells (mouse preadipocyte cell line), mouse BMDMs, and Caco-2 that had been pretreated with or without 15 μM Bith, and cellular fluorescence was analyzed at the 10 min time point (Fig. 5). In all four cell types, Bith inhibited flame-NAPE cellular fluorescence to a greater extent than PED-A1 cellular fluorescence (47% vs. 37% inhibition in HEK293%; 78% vs. 55% in 3T3-L1; 82% vs. 72% in BMDM; and 54% vs. 39% in Caco-2). These results are consistent with flame-NAPE cellular fluorescence selectively reporting NAPE-PLD activity and PED-A1 cellular fluorescence reporting the combined activity of NAPE-PLD and PLA₁.

DISCUSSION

Our results demonstrate that the use of flame-NAPE provides a facile method to selectively assay NAPE-PLD activity in a variety of cell types. Such an assay has long been needed to enable studies elucidating how various external stimuli and signaling pathways modulate NAPE-PLD activity and NAE biosynthesis. Understanding control of NAE biosynthesis is critical because NAEs including AEA, PEA, and OEA regulate a host of physiological processes, including feeding behavior, nociception, leukocyte infiltration, insulin secretion,

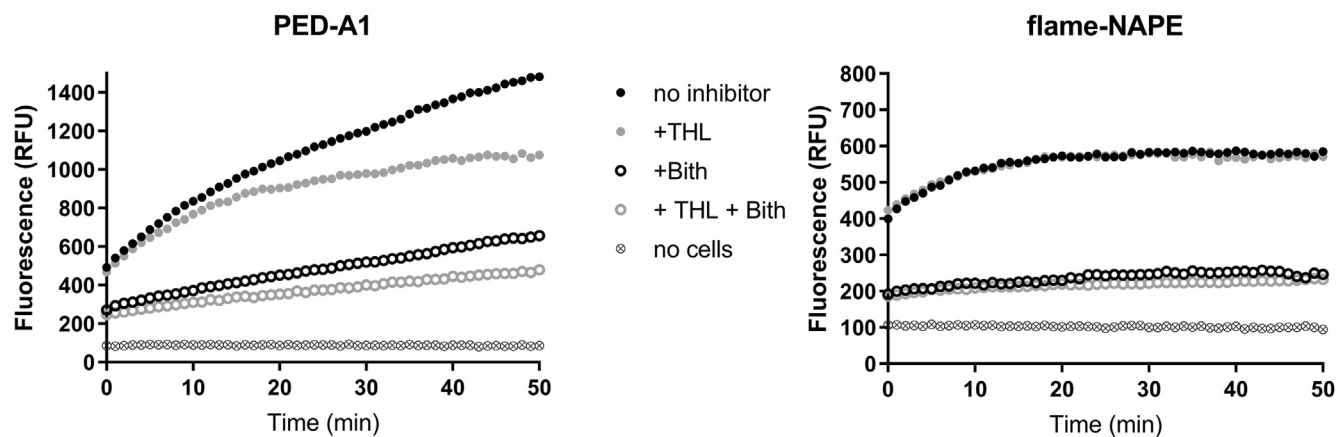


Fig. 4. Phospholipase activity in HepG2 cells measured using flame-NAPE is sensitive to NAPE-PLD inhibition but not PLA₁ inhibition, whereas phospholipase activity measured by PED-A1 is sensitive to both. HepG2 cells in 96-well plates were treated with 10 μM tetrahydrolipstatin (THL, a pan-lipase inhibitor) and/or 15 μM bithionol (Bith, an NAPE-PLD inhibitor) prior to the addition of either PED-A1 or flame-NAPE (4 μM). Representative 50 min fluorescence time course (1 read per minute) for each treatment. Similar time course obtained on two separate days. Symbols represent average of 6–8 replicate wells for each treatment.

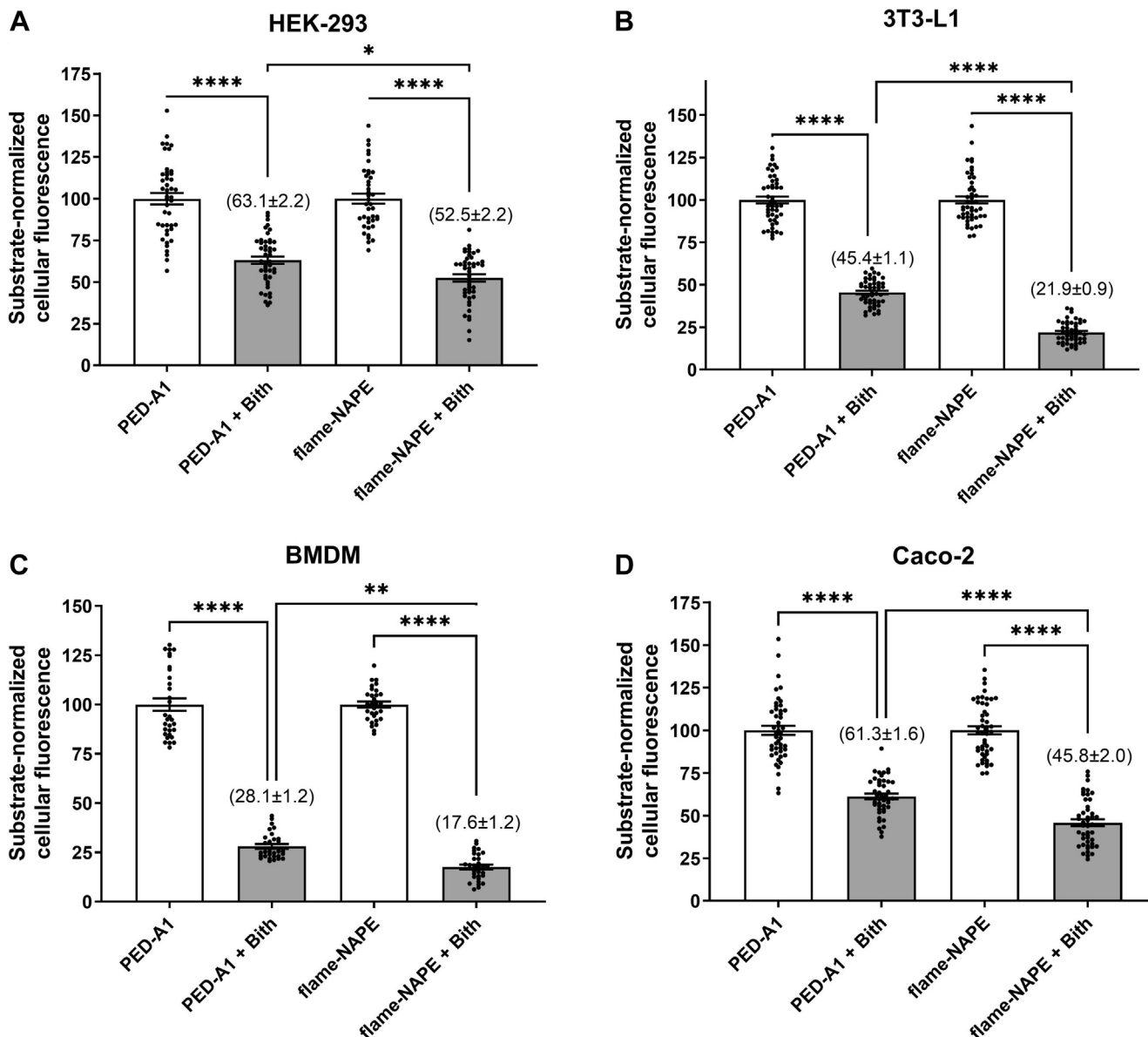


Fig. 5. Phospholipase activity measured using flame-NAPE is more sensitive to NAPE-PLD inhibition than activity measured using PED-A1 in many cell types. Various cultured cell types were treated with or without 15 μ M bithionol (Bith), an NAPE-PLD inhibitor, prior to incubation with PED-A1 or flame-NAPE (4 μ M). Bars represent average \pm SEM, $n = 31$ –48 with 7–16 replicates each for three separate experimental days. A: HEK-293, (B) 3T3-L1, (C) BMDM (bone marrow-derived macrophage), and (D) Caco-2. One-way ANOVA for each cell type $P < 0.0001$, Tukey multiple comparisons test, $*P < 0.025$, $**P < 0.0013$, and $****P < 0.0001$. Number in parentheses equals substrate-normalized cellular fluorescence for Bith-treated cells (mean \pm SEM).

and macrophage polarization (4–11); therefore, reduced activity of their biosynthetic enzymes may be important factors in disease.

Understanding how NAE biosynthesis is regulated and why it becomes dysregulated under some conditions has been challenging in part because of the lack of appropriate probes and associated methods to measure the activity of individual NAE biosynthetic enzymes. In addition to NAPE-PLD, at least two other enzymes act on NAPE. ABHD4 acts as a PLA₁ and PLA₂ to convert NAPE to GP-NAE (19), which can be converted to NAE by GDE1 or GDE4 or other similar phosphodiesterases (6, 15, 16). Genetic deletion of *Abhd4* in mice demonstrates that this NAE biosynthetic

enzyme plays a critical role in developmental anoxia (47). *Abhd4* deletion in mice does not significantly decrease their brain levels of AEA, OEA, PEA, or their precursor NAPEs, but does reduce levels of GP-NAEs (48). To the best of our knowledge, the effects of *Abhd4* deletion on NAE levels in tissues other than brain have not been reported. Another alternative pathway for NAE biosynthesis utilizes an unidentified NAPE-hydrolyzing phospholipase C (NAPE-PLC) that hydrolyzes NAPE to diacylglycerol and phospho-NAE. Phospho-NAE can then be converted to NAE via phosphatases such as PTPN22 (49). Lipopolysaccharide stimulation of macrophages decreases expression of NAPE-PLD (20, 49) and reduces levels of PEA (20, 50)

and OEA (50) but increases levels of AEA (49–51) and phospho-AEA (49). These results suggest that unlike NAPE-PLD, the putative NAPE-PLC preferentially utilizes *N*-arachidonyl-PE over *N*-palmitoyl-PE or *N*-oleoyl-PE and might therefore control AEA levels. However, genetic deletion of *Nape-pld* does reduce levels of AEA as well as PEA and OEA in brain (52, 53), so control of AEA biosynthesis likely depends on multiple pathways (54). Therefore, the straightforward assay method to measure NAPE-PLD activity we report here should be helpful in better understanding how this enzyme controls levels of AEA, OEA, and PEA.

Fluorogenic activity assays have considerable advantages in terms of reduced time and resource consumption compared with methods such as TLC and LC/MS/MS, as long as the probes utilized selectively measure the desired activity. While the fluorogenic probes PED6 and PED-A1 have been used in high-throughput screening to identify NAPE-PLD inhibitors *in vitro* (22, 27, 28), they are sensitive to hydrolysis by other phospholipases likely to be present in cells and tissues. PED6 was originally created as a probe for PLA₂ activity (23), whereas PED-A1 was created as a probe for PLA₁ activity (26). Since ABHD4 has both PLA₁ and PLA₂ activity, neither PED-A1 nor PED6 can readily distinguish between NAPE-PLD and ABHD4 activity. Many other PLA₁s or PLA₂s that can hydrolyze PED-A1 and PED6 are present in cells and tissue where measurement of NAPE-PLD activity is of interest. For instance, PED-A1 has been used to measure the PLA₁ activity of endothelial lipase in human umbilical vein endothelial cells (26). Other mammalian PLA₁s include hepatic lipase, phosphatidylserine-specific PLA₁, membrane-associated phosphatidic acid-selective PLA₁α/β, pancreatic lipase-related protein 2, and phospholipase A/acyltransferase-2 (55, 56). Our studies with THL, a pan-inhibitor of serine hydrolase-type lipases, confirm that a significant portion of PED-A1 fluorescence measured in cultured cells results from phospholipase activity other than NAPE-PLD activity, particularly at longer end points. THL markedly reduced PED-A1 fluorescence in HepG2 cells, while having no effect on flame-NAPE fluorescence. Furthermore, in all the cell types we tested, the NAPE-PLD inhibitor (Bith) decreased PED-A1 cellular fluorescence to a lesser extent than it decreased flame-NAPE cellular fluorescence. Thus, if PED-A1 (or PED6) fluorescence is used to measure NAPE-PLD activity in cultured cells or tissues, THL (or another appropriate inhibitor) should be added prior to initiation of the assay to block serine hydrolase-type lipases, and the end point of the assay should be relatively short (i.e., 10 min).


Use of flame-NAPE to measure NAPE-PLD activity in our assay method overcomes the major limitations of PED-A1 and PED6. Substituting an *N*-methyl amide group at the *sn*-1 ester bond made flame-NAPE completely resistant to hydrolysis by *A. oryzae* Pla₁, unlike PED-A1 that was entirely hydrolyzed by this

enzyme. Flame-NAPE fluorescence was not inhibited by THL in HepG2 cells, supporting the notion that serine hydrolase-type phospholipases do not significantly contribute to flame-NAPE hydrolysis. Flame-NAPE fluorescence was significantly inhibited by 15 μM Bith in all the cell types we tested. It is possible that in some cell types, a nonserine hydrolase-type phospholipase such as the putative NAPE-PLC contributes to flame-NAPE cellular fluorescence. One limitation of our validation studies is that the contribution of the putative NAPE-PLC to flame-NAPE fluorescence cannot be tested directly because it has not been cloned or purified. However, significant NAPE-PLC contribution seems unlikely because this putative NAPE-PLC appears to prefer *N*-arachidonyl-PE over NAPEs with shorter saturated *N*-acyl chains (49), likely making flame-NAPE a poor NAPE-PLC substrate.

Although the method we report here is to measure relative NAPE-PLD activity in cultured cells, the previous use of PED6 in zebrafish embryo and larvae to image sites of active pla₂ in the digestive tract (25, 57) suggest that flame-NAPE could be used in a similar manner for imaging active *nape-pld*. This might be particularly useful for examining the effects of diet and other environmental factors on intestinal, adipocyte, or macrophage *nape-pld* activity. Imaging of the flame-NAPE could also provide insight into changes in NAPE-PLD localization within cultured cells, although potential diffusion of the BODIPY-phosphatidic acid from its initial site of formation must be considered.

In summary, using flame-NAPE provides a rapid and straightforward method to selectively assay NAPE-PLD activity that should facilitate studies to identify factors that alter NAPE-PLD activity, the role of NAPE-PLD activity in controlling individual levels of NAEs, whether changes in NAPE-PLD activity contribute to disease, and the extent to which potential interventions rescue NAPE-PLD activity.

Data availability

Processed data generated during this study are included in the published article and its supplemental data files. The raw and processed data for these studies are archived at the FigShare repository Web site <https://doi.org/10.6084/m9.figshare.17035610>. 

Supplemental data




This article contains [supplemental data](#) (58–60).

Author contributions

G. A. S. and S. S. D. conceptualization; J. E. Z., J. T., B. D., K. K., G. A. S., and S. S. D. methodology; J. E. Z. validation; J. E. Z. and S. S. D. formal analysis; J. E. Z., J. T., B. D., K. K., A. C. D., and S. S. D. investigation; G. A. S. and S. S. D. resources; S. S. D. data curation; J. E. Z. and S. S. D. writing—original draft; J. E. Z., K. K., A. C. D., G. A. S., and S. S. D. writing—review and editing; G. A. S. and S. S. D.

visualization; G. A. S. and S. S. D. supervision; S. S. D. project administration; G. A. S. and S. S. D. funding acquisition.

Author ORCIDs

Jonah E. Zarrow  <https://orcid.org/0000-0003-2536-2297>
Amanda C. Doran  <https://orcid.org/0000-0002-1576-6274>
Sean S. Davies  <https://orcid.org/0000-0001-9879-8062>

Funding and additional information

This work was supported in part by funds from the National Heart Lung Blood Institute P01HL116263 (to S. S. D. and A. C. D.); the National Institute of General Medical Science T32GM065086 (to J. E. Z.); the American Heart Association (fellowship no. 835504, to J. E. Z. and grant no. 17FTF33660643, to A. C. D.); the Molecular Design and Synthesis Center at the Vanderbilt University (to J. T., B. D., K. K., and G. A. S.); the Vanderbilt Diabetes Center Institutional Discovery Grant (to S. S. D.); the Department of Pharmacology at the Vanderbilt University (to S. S. D.); and the Department of Medicine at Vanderbilt University Medical Center (to A. C. D.).

Conflict of interest

The authors declare that they have no conflicts of interest with the contents of this article.

Abbreviations

ABHD4, alpha/beta-hydrolase-4; AEA, *N*-arachidonylethanolamide; Bith, bithionol; BMDM, bone marrow-derived macrophage; GP-NAE, glycerophospho-NAE; HEK293, human embryonic kidney 293 cell line; NAE, *N*-acyl-ethanolamide; NAPE, *N*-acyl-phosphatidylethanolamine; OEA, *N*-oleoyl-ethanolamide; PEA, *N*-palmitoyl-ethanolamide; PLC, phospholipase C; PLD, phospholipase D; THL, tetrahydrolipstatin.

Manuscript received June 10, 2021, and in revised form November 17, 2021. Published, JLR Papers in Press, November 26, 2021, <https://doi.org/10.1016/j.jlr.2021.100156>

REFERENCES

- Okamoto, Y., Morishita, J., Tsuboi, K., Tonai, T., and Ueda, N. (2004) Molecular characterization of a phospholipase D generating anandamide and its congeners. *J. Biol. Chem.* **279**, 5298–5305
- Di Marzo, V., Goparaju, S. K., Wang, L., Liu, J., Batkai, S., Jarai, Z., Fezza, F., Miura, G. I., Palmieri, R. D., Sugiura, T., and Kunos, G. (2001) Leptin-regulated endocannabinoids are involved in maintaining food intake. *Nature* **410**, 822–825
- Liu, Q., Tonai, T., and Ueda, N. (2002) Activation of *N*-acylethanolamine-releasing phospholipase D by polyamines. *Chem. Phys. Lipids* **115**, 77–84
- Fu, J., Gaetani, S., Oveisi, F., Lo Verme, J., Serrano, A., Rodriguez De Fonseca, F., Rosengarth, A., Luecke, H., Di Giacomo, B., Tarzia, G., and Piomelli, D. (2003) Oleyethanolamide regulates feeding and body weight through activation of the nuclear receptor PPAR- α . *Nature* **425**, 90–93
- Lo Verme, J., Fu, J., Astarita, G., La Rana, G., Russo, R., Calignano, A., and Piomelli, D. (2005) The nuclear receptor peroxisome proliferator-activated receptor- α mediates the anti-inflammatory actions of palmitoylethanolamide. *Mol. Pharmacol.* **67**, 15–19
- Hussain, Z., Uyama, T., Tsuboi, K., and Ueda, N. (2017) Mammalian enzymes responsible for the biosynthesis of *N*-acylethanolamines. *Biochim. Biophys. Acta Mol. Cell Biol. Lipids* **1862**, 1546–1561
- Rinne, P., Guillamat-Prats, R., Rami, M., Bindila, L., Ring, L., Lyytikäinen, L. P., Raitoharju, E., Oksala, N., Lehtimäki, T., Weber, C., van der Vorst, E. P. C., and Steffens, S. (2018) Palmitoylethanolamide promotes a proresolving macrophage phenotype and attenuates atherosclerotic plaque formation. *Arterioscler. Thromb. Vasc. Biol.* **38**, 2562–2575
- Moran, B. M., Abdel-Wahab, Y. H., Flatt, P. R., and McKillop, A. M. (2014) Activation of GPR119 by fatty acid agonists augments insulin release from clonal beta-cells and isolated pancreatic islets and improves glucose tolerance in mice. *Biol. Chem.* **395**, 453–464
- Ning, Y., O'Neill, K., Lan, H., Pang, L., Shan, L. X., Hawes, B. E., and Hedrick, J. A. (2008) Endogenous and synthetic agonists of GPR119 differ in signalling pathways and their effects on insulin secretion in MIN6c4 insulinoma cells. *Br. J. Pharmacol.* **155**, 1056–1065
- Di Paola, R., Impellizzeri, D., Mondello, P., Velardi, E., Aloisi, C., Cappellani, A., Esposito, E., and Cuzzocrea, S. (2012) Palmitoylethanolamide reduces early renal dysfunction and injury caused by experimental ischemia and reperfusion in mice. *Shock* **38**, 356–366
- Corcoran, L., Roche, M., and Finn, D. P. (2015) The role of the brain's endocannabinoid system in pain and its modulation by stress. *Int. Rev. Neurobiol.* **125**, 203–255
- Petersen, G., and Hansen, H. S. (1999) *N*-acylphosphatidylethanolamine-hydrolysing phospholipase D lacks the ability to transphosphatidylate. *FEBS Lett.* **455**, 41–44
- Simon, G. M., and Cravatt, B. F. (2010) Characterization of mice lacking candidate *N*-acyl ethanolamine biosynthetic enzymes provides evidence for multiple pathways that contribute to endocannabinoid production in vivo. *Mol. Biosyst.* **6**, 1411–1418
- Okamoto, Y., Wang, J., Morishita, J., and Ueda, N. (2007) Biosynthetic pathways of the endocannabinoid anandamide. *Chem. Biodivers.* **4**, 1842–1857
- Tsuboi, K., Okamoto, Y., Rahman, I. A. S., Uyama, T., Inoue, T., Tokumura, A., and Ueda, N. (2015) Glycerophosphodiesterase GDE4 as a novel lysophospholipase D: a possible involvement in bioactive *N*-acylethanolamine biosynthesis. *Biochim. Biophys. Acta Mol. Cell Biol. Lipids* **1851**, 537–548
- Simon, G. M., and Cravatt, B. F. (2008) Anandamide biosynthesis catalyzed by the phosphodiesterase GDE1 and detection of glycerophospho-*N*-acyl ethanolamine precursors in mouse brain. *J. Biol. Chem.* **283**, 9341–9349
- Petersen, G., Pedersen, A. H., Pickering, D. S., Begtrup, M., and Hansen, H. S. (2009) Effect of synthetic and natural phospholipids on *N*-acylphosphatidylethanolamine-hydrolysing phospholipase D activity. *Chem. Phys. Lipids* **162**, 53–61
- Diep, T. A., Madsen, A. N., Holst, B., Kristiansen, M. M., Wellner, N., Hansen, S. H., and Hansen, H. S. (2011) Dietary fat decreases intestinal levels of the anorectic lipids through a fat sensor. *FASEB J.* **25**, 765–774
- Simon, G. M., and Cravatt, B. F. (2006) Endocannabinoid biosynthesis proceeding through glycerophospho-*N*-acyl ethanolamine and a role for alpha/beta-hydrolase 4 in this pathway. *J. Biol. Chem.* **281**, 26465–26472
- Zhu, C., Solorzano, C., Sahar, S., Realini, N., Fung, E., Sassone-Corsi, P., and Piomelli, D. (2011) Proinflammatory stimuli control *N*-acylphosphatidylethanolamine-specific phospholipase D expression in macrophages. *Mol. Pharmacol.* **79**, 786–792
- Fu, J., Astarita, G., Gaetani, S., Kim, J., Cravatt, B. F., Mackie, K., and Piomelli, D. (2007) Food intake regulates oleyethanolamide formation and degradation in the proximal small intestine. *J. Biol. Chem.* **282**, 1518–1528
- Mock, E. D., Mustafa, M., Gunduz-Cinar, O., Cinar, R., Petrie, G. N., Kantae, V., Di, X., Ogasawara, D., Varga, Z. V., Palocz, J., Miliano, C., Donvito, G., van Esbroeck, A. C. M., van der Gracht, A. M. F., Kotsogianni, I., et al. (2020) Discovery of a NAPE-PLD inhibitor that modulates emotional behavior in mice. *Nat. Chem. Biol.* **16**, 667–675
- Hendrickson, H. S., Hendrickson, E. K., Johnson, I. D., and Farber, S. A. (1999) Intramolecularly quenched BODIPY-labeled phospholipid analogs in phospholipase A2 and platelet-activating factor acetylhydrolase assays and in vivo fluorescence imaging. *Anal. Biochem.* **276**, 27–35
- Leu, B. H., and Schmidt, J. T. (2008) Arachidonic acid as a retrograde signal controlling growth and dynamics of retinotectal arbors. *Dev. Neurobiol.* **68**, 18–30

25. Hama, K., Provost, E., Baranowski, T. C., Rubinstein, A. L., Anderson, J. L., Leach, S. D., and Farber, S. A. (2009) In vivo imaging of zebrafish digestive organ function using multiple quenched fluorescent reporters. *Am. J. Physiol. Gastrointest. Liver Physiol.* **296**, G445–G453
26. Darrow, A. L., Olson, M. W., Xin, H., Burke, S. L., Smith, C., Schalk-Hihi, C., Williams, R., Bayoumy, S. S., Deckman, I. C., Todd, M. J., Damiano, B. P., and Connelly, M. A. (2011) A novel fluorogenic substrate for the measurement of endothelial lipase activity. *J. Lipid Res.* **52**, 374–382
27. Aggarwal, G., Zarrow, J. E., Mashhadi, Z., Flynn, C. R., Vinson, P., Weaver, C. D., and Davies, S. S. (2020) Symmetrically substituted dichlorophenes inhibit N-acyl-phosphatidylethanolamine phospholipase D. *J. Biol. Chem.* **295**, 7289–7300
28. Mock, E. D., Kotsogianni, I., Driever, W. P. F., Fonseca, C. S., Vooijs, J. M., den Dulk, H., van Boeckel, C. A. A., and van der Stelt, M. (2021) Structure-activity relationship studies of pyrimidine-4-carboxamides as inhibitors of N-acylphosphatidylethanolamine phospholipase D. *J. Med. Chem.* **64**, 481–515
29. Pasternack, S. M., von Kugelgen, I., Muller, M., Oji, V., Traupe, H., Sprecher, E., Nothen, M. M., Janecke, A. R., and Betz, R. C. (2009) In vitro analysis of LIPH mutations causing hypotrichosis simplex: evidence confirming the role of lipase H and lysophosphatidic acid in hair growth. *J. Invest. Dermatol.* **129**, 2772–2776
30. Asano, A., Nelson-Harrington, J. L., and Travis, A. J. (2013) Phospholipase B is activated in response to sterol removal and stimulates acrossome exocytosis in murine sperm. *J. Biol. Chem.* **288**, 28104–28115
31. Kuge, H., Akahori, K., Yagyu, K. I., and Honke, K. (2014) Functional compartmentalization of the plasma membrane of neurons by a unique acyl chain composition of phospholipids. *J. Biol. Chem.* **289**, 26783–26793
32. Doran, A. C., Ozcan, L., Cai, B., Zheng, Z., Fredman, G., Rymond, C. C., Dorweiler, B., Sluimer, J. C., Hsieh, J., Kuriakose, G., Tall, A. R., and Tabas, I. (2017) CAMKIIgamma suppresses an efferocytosis pathway in macrophages and promotes atherosclerotic plaque necrosis. *J. Clin. Invest.* **127**, 4075–4089
33. Hauptman, J. B., Jeunet, F. S., and Hartmann, D. (1992) Initial studies in humans with the novel gastrointestinal lipase inhibitor Ro 18-0647 (tetrahydrolipstatin). *Am. J. Clin. Nutr.* **55**, 309S–313S
34. Fernandez, E., and Borgström, B. (1989) Effects of fat from the intestine of the rat. *Biochim. Biophys. Acta.* **1001**, 249–255
35. Hogan, S., Fleury, A., Hadvary, P., Lengsfeld, H., Meier, M. K., Triscari, J., and Sullivan, A. C. (1987) Studies on the antiobesity activity of tetrahydrolipstatin, a potent and selective inhibitor of pancreatic lipase. *Int. J. Obes.* **11 Suppl 3**, 35–42
36. Tatematsu, S., Francis, S. A., Natarajan, P., Rader, D. J., Saghatelian, A., Brown, J. D., Michel, T., and Plutzky, J. (2013) Endothelial lipase is a critical determinant of high-density lipoprotein-stimulated sphingosine 1-phosphate-dependent signaling in vascular endothelium. *Arterioscler. Thromb. Vasc. Biol.* **33**, 1788–1794
37. Rinninger, F., Mann, W. A., Kaiser, T., Ahle, S., Meyer, N., and Greten, H. (1998) Hepatic lipase mediates an increase in selective uptake of high-density lipoprotein-associated cholesteryl esters by human Hep 3B hepatoma cells in culture. *Atherosclerosis.* **141**, 273–285
38. Everard, A., Plovier, H., Rastelli, M., Van Hul, M., de Wouters d'Oplinter, A., Geurts, L., Druart, C., Robine, S., Delzenne, N. M., Muccioli, G. G., de Vos, W. M., Luquet, S., Flamand, N., Di Marzo, V., and Cani, P. D. (2019) Intestinal epithelial N-acylphosphatidylethanolamine phospholipase D links dietary fat to metabolic adaptations in obesity and steatosis. *Nat. Commun.* **10**, 457
39. Geurts, L., Everard, A., Van Hul, M., Essaghir, A., Duparc, T., Matamoros, S., Plovier, H., Castel, J., Denis, R. G., Bergiers, M., Druart, C., Alhouayek, M., Delzenne, N. M., Muccioli, G. G., Demoulin, J. B., et al. (2015) Adipose tissue NAPE-PLD controls fat mass development by altering the browning process and gut microbiota. *Nat. Commun.* **6**, 6495
40. Chen, Z., Zhang, Y., Guo, L., Dosoky, N., de Ferra, L., Peters, S., Niswender, K. D., and Davies, S. S. (2017) Leptogenic effects of NAPE require activity of NAPE-hydrolyzing phospholipase D. *J. Lipid Res.* **58**, 1624–1635
41. Fu, J., Kim, J., Oveisi, F., Astarita, G., and Piomelli, D. (2008) Targeted enhancement of oleoylethanolamide production in proximal small intestine induces across-meal satiety in rats. *Am. J. Physiol. Regul. Integr. Comp. Physiol.* **295**, R45–R50
42. Ueda, N., Okamoto, Y., and Tsuboi, K. (2005) Endocannabinoid-related enzymes as drug targets with special reference to N-acylphosphatidylethanolamine-hydrolyzing phospholipase D. *Curr. Med. Chem.* **12**, 1413–1422
43. Yun, C. C., and Kumar, A. (2015) Diverse roles of LPA signaling in the intestinal epithelium. *Exp. Cell Res.* **333**, 201–207
44. Richmond, G. S., and Smith, T. K. (2011) Phospholipases A(1). *Int. J. Mol. Sci.* **12**, 588–612
45. Lopategi, A., Lopez-Vicario, C., Alcaraz-Quiles, J., Garcia-Alonso, V., Rius, B., Titos, E., and Claria, J. (2016) Role of bioactive lipid mediators in obese adipose tissue inflammation and endocrine dysfunction. *Mol. Cell. Endocrinol.* **419**, 44–59
46. Lee, J. H., Kim, D., Oh, Y. S., and Jun, H. S. (2019) Lysophosphatidic acid signaling in diabetic nephropathy. *Int. J. Mol. Sci.* **20**, 2850
47. László, Z. I., Lele, Z., Zöldi, M., Miczán, V., Mógor, F., Simon, G. M., Mackie, K., Kacsokovics, I., Cravatt, B. F., and Katona, I. (2020) ABHD4-dependent developmental anokis safeguards the embryonic brain. *Nat. Commun.* **11**, 4363
48. Lee, H.-C., Simon, G. M., and Cravatt, B. F. (2015) ABHD4 regulates multiple classes of N-acyl phospholipids in the mammalian central nervous system. *Biochemistry.* **54**, 2539–2549
49. Liu, J., Wang, L., Harvey-White, J., Osei-Hyiaman, D., Razdan, R., Gong, Q., Chan, A. C., Zhou, Z., Huang, B. X., Kim, H.-Y., and Kunos, G. (2006) A biosynthetic pathway for anandamide. *Proc. Natl. Acad. Sci. U. S. A.* **103**, 13345–13350
50. Jin, W., Yang, L., Yi, Z., Fang, H., Chen, W., Hong, Z., Zhang, Y., Zhang, G., and Li, L. (2020) Anti-inflammatory effects of fucoxanthinol in LPS-induced RAW264.7 cells through the NAAA-PEA pathway. *Mar. Drugs.* **18**, 222
51. Liu, J., Batkai, S., Pacher, P., Harvey-White, J., Wagner, J. A., Cravatt, B. F., Gao, B., and Kunos, G. (2003) Lipopolysaccharide induces anandamide synthesis in macrophages via CD14/MAPK/phosphoinositide 3-kinase/kappaB independently of platelet-activating factor. *J. Biol. Chem.* **278**, 45034–45039
52. Leishman, E., Mackie, K., Luquet, S., and Bradshaw, H. B. (2016) Lipidomics profile of a NAPE-PLD KO mouse provides evidence of a broader role of this enzyme in lipid metabolism in the brain. *Biochim. Biophys. Acta Mol. Cell Biol. Lipids.* **1861**, 491–500
53. Tsuboi, K., Okamoto, Y., Ikematsu, N., Inoue, M., Shimizu, Y., Uyama, T., Wang, J., Deutsch, D. G., Burns, M. P., Ulloa, N. M., Tokumura, A., and Ueda, N. (2011) Enzymatic formation of N-acylethanolamines from N-acylethanolamine plasmalogen through N-acylphosphatidylethanolamine-hydrolyzing phospholipase D-dependent and -independent pathways. *Biochim. Biophys. Acta Mol. Cell Biol. Lipids.* **1811**, 565–577
54. Leung, D., Saghatelian, A., Simon, G. M., and Cravatt, B. F. (2006) Inactivation of N-acyl phosphatidylethanolamine phospholipase D reveals multiple mechanisms for the biosynthesis of endocannabinoids. *Biochemistry.* **45**, 4720–4726
55. Aoki, J., Inoue, A., Makide, K., Saiki, N., and Arai, H. (2007) Structure and function of extracellular phospholipase A1 belonging to the pancreatic lipase gene family. *Biochimie.* **89**, 197–204
56. Uyama, T., Ikematsu, N., Inoue, M., Shinohara, N., Jin, X.-H., Tsuboi, K., Tonai, T., Tokumura, A., and Ueda, N. (2012) Generation of N-acylphosphatidylethanolamine by members of the phospholipase A/acyltransferase (PLA/AT) family. *J. Biol. Chem.* **287**, 31905–31919
57. Farber, S. A., Pack, M., Ho, S.-Y., Johnson, I. D., Wagner, D. S., Dosch, R., Mullins, M. C., Hendrickson, H. S., Hendrickson, E. K., and Halpern, M. E. (2001) Genetic analysis of digestive physiology using fluorescent phospholipid reporters. *Science.* **292**, 1385–1388
58. Kalhor-Monfared, S., Beauvineau, C., Scherman, D., and Girard, C. (2016) Synthesis and cytotoxicity evaluation of aryl triazolic derivatives and their hydroxymethine homologues against B16 melanoma cell line. *Eur. J. Med. Chem.* **122**, 436–441
59. Doboszewski, B., Groaz, E., and Herdewijn, P. (2013) Synthesis of phosphonoglycine backbone units for the development of phosphono peptide nucleic acids. *Eur. J. Org. Chem.* **122**, 4804–4815
60. Ferguson, C., Prestwich G., Madan D. Fluorogenic assay for lysophospholipase D activity using fluorogenic lysophospholipid derivatives as substrates, and diagnostic and screening applications. United States, US20100260682 A1